



A CFD-Model for prediction of unintended porosities in metal matrix composites

A preliminary study

Li, Shizhao; Spangenberg, Jon; Hattel, Jesper Henri

Published in:

Proceedings of the 19th international conference on composite materials

Publication date:

2013

[Link back to DTU Orbit](#)

Citation (APA):

Li, S., Spangenberg, J., & Hattel, J. H. (2013). A CFD-Model for prediction of unintended porosities in metal matrix composites: A preliminary study. In *Proceedings of the 19th international conference on composite materials* (pp. 1625-1632). ICCM19 Secretariat.

General rights

Copyright and moral rights for the publications made accessible in the public portal are retained by the authors and/or other copyright owners and it is a condition of accessing publications that users recognise and abide by the legal requirements associated with these rights.

- Users may download and print one copy of any publication from the public portal for the purpose of private study or research.
- You may not further distribute the material or use it for any profit-making activity or commercial gain
- You may freely distribute the URL identifying the publication in the public portal

If you believe that this document breaches copyright please contact us providing details, and we will remove access to the work immediately and investigate your claim.

A CFD-MODEL FOR PREDICTION OF UNINTENDED POROSITIES IN METAL MATRIX COMPOSITES: A PRELIMINARY STUDY

S. Li^{1*}, J. Spangenberg¹, J. H. Hattel¹

¹ Mechanical Engineering Department, Technical University of Denmark (DTU), Kgs. Lyngby, Denmark

* Corresponding author (shili@mek.dtu.dk)

Keywords: *infiltration process, metal-matrix composites, porosity distribution, CFD model*

1 Introduction

Metal-matrix composites (MMCs) are materials with great potential in applications for many industries, e.g. automotive, electronics, aviation, and aerospace, due to their excellent properties, such as high damping capacity, high specific strength, low thermal expansion coefficient, and low weight [1].

A common method used for fabrication of MMCs is the pressure infiltration process [2-8], which consists of injecting molten metal into a preform under an external pressure. However, experimental investigations in literature report that the fabrication process is a delicate matter, which often results in incomplete infiltration [1, 9-10].

Numerical modeling can be a theoretical tool to provide very useful information on the general behavior of the infiltration process and potentially reduce the experimental work related to obtaining optimized process parameters. Previous published numerical studies on the pressure infiltration process are at present very limited. The few existing studies primarily focus on the global propagation of the fully and non-fully saturated regions by considering the mass balance equation together with Darcy's law [11-16]. The drawback of these porous media/permeability approaches is the disability of capturing one of the key fabrication errors which is the unintended porosities at the end of the process.

This paper presents a numerical method that simulates the flow through the porous corridors of the preform, which in theory enables the prediction of unintended porosities at the end of the process.

However, the obstacle for this new approach is that the size of the preform in this process is usually of the order of 5-10cm in each direction, while the size of the reinforcement (fibers or spherical particles) is of the order 10-100 μ m and that combination leads to a very calculation-heavy numerical model, since the control volume in the mesh at least needs to be at the same length scale as the reinforcement. Therefore, the objective of this paper is to evaluate the potential for this numerical approach to predict unintended porosities in metal matrix composites with special emphasis on fiber vs. domain sizes.

In the first part of the paper, the three-dimensional Computational Fluid Dynamics (CFD) model is presented together with a description of the preform. In the second part the infiltration results are reported and compared with porous media/permeability approach based results from literature. Finally, the pros and cons for this CFD approach are discussed.

2 Numerical Model

2.1 Governing Equations

The flow of the molten metal during the infiltration of the preform is a highly non-linear problem. The two main physical phenomena in this process are the flow and solidification of the molten metal. In this study the flow of the molten metal is of focus, thus isothermal calculations are conducted. In addition, the molten metal is considered as an incompressible Newtonian fluid.

The global Newtonian flow is captured by solving the mass continuity equation given in Eqn. 1

together with the momentum equations given in Eqn. 2.

$$\nabla \mathbf{u} = 0 \quad (1)$$

$$\rho \left(\frac{\partial \mathbf{u}}{\partial t} + \mathbf{u} \cdot \nabla \mathbf{u} \right) = -\nabla p + \mu \nabla^2 \mathbf{u} \quad (2)$$

where u is the velocity of the molten metal, ρ is the density, t is the time, and p is the pressure. Note that no gravitational force, surface tension or pore pressure are considered in this study.

2.2 CFD solver

The commercial software FLOW-3D is used to calculate the incompressible Newtonian flow of the molten metal [17]. FLOW-3D is a CFD software capable of analyzing various physical flow processes. In this study, the software solves Eqn. 1 and 2 by the usage of the Finite Volume Method (FVM). The pressure and velocity fields are found on a staggered grid by the Generalized Minimum Residual Solver (GMRES). In addition, the software utilizes an explicit Volume Of Fluid (VOF) algorithm to track the free surface of the molten metal.

2.3 Description of the CFD model

The material properties, the geometry of the mold, and the boundary conditions utilized in this study are adopted from [11] in order to carry out a comparison with results from where the porous media/permeability approach is utilized. The molten metal is considered to be an aluminum alloy A380 with a dynamic viscosity of 0.0012 Pa·s and a density of $2.46 \times 10^3 \text{ kg/m}^3$, while the material of the fibers is assumed to be ceramic. These are common materials used to produce metal matrix composites by an infiltration process. The geometry of the mold is a cylinder with a diameter of 10 cm and a height of 3 cm, see Fig. 1. Inside the mold a porous preform is placed (description follows in section 2.4). At the top of the cylinder, a circular inlet is positioned with a diameter of 15mm which allows the molten metal to flow into the mold and penetrate the porous preform. The boundary condition at the inlet is a pressure of 0.8MPa. Furthermore, a no-slip (zero velocity) boundary condition is used at the wall of the mold and surface of the fibrous preform.

Finally, two symmetry boundary conditions are used between the red and grey/blue part of the domain, shown in Fig. 1, which enables only one fourth of the preform to be simulated thereby reducing the calculation time.

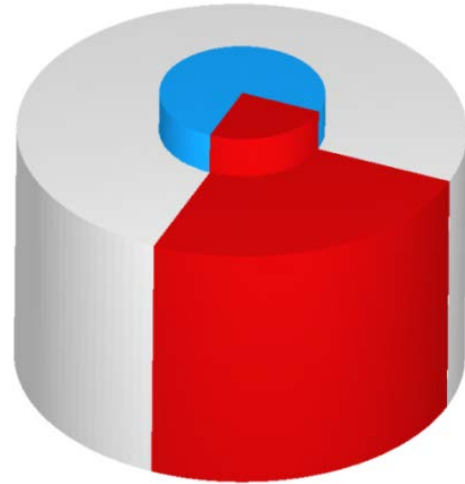


Fig. 1. Schematic view of preform and inlet. The red subdomain represents the part of the geometry simulated by the numerical model.

2.4 Geometric Model of Porous Preform

The geometry and size of the porous preform are the same as the mold's. The porous structure is generated based on the following three assumptions:

1. The preform consists of many fiber layers positioned in a staggered manner.
2. The shape of each fiber layer is similar to a net, which is represented by a number of orthogonal straight fibers.
3. The cross-section of the individual fibers is squared.

The steps involved in processing the geometrical information of the porous preform are: generating one fiber layer, generating the whole preform, and importing the preform into FLOW-3D. Each of the steps is detailed described in the next three sections.

2.4.1 Generating one fiber layer

One fiber layer consists of many fiber units. In Fig. 2, a 3-dimensional image of one fiber unit is shown. This fiber unit is generated with a MATLAB code. First, a Boolean matrix with entries of 0 and 1 is conducted. In this matrix, “0” represents the fraction of air, and “1” represents for the fraction of fiber. Then, the function STLWRITE [18] is called to generate the Stereo Lithography (STL) file based on the Boolean matrix. The total length of the fiber unit is five times the thickness of the cross-section.

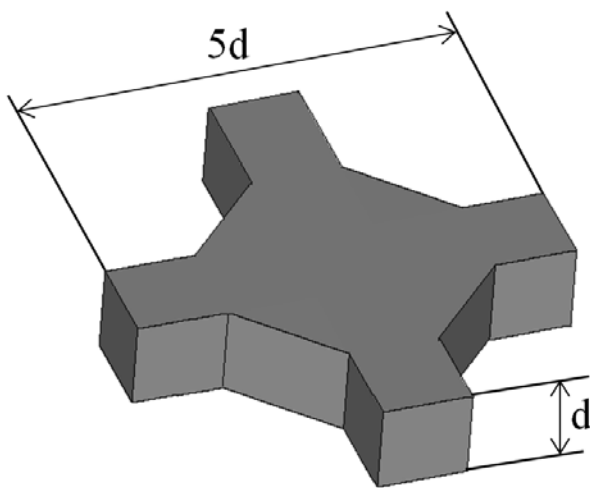


Fig. 2. 3-D image of one unit in the fiber layer

Afterwards, the fiber unit is copied and distributed in order to generate the fiber layer seen in Fig. 3. Finally, an STL file of one fiber layer is created.

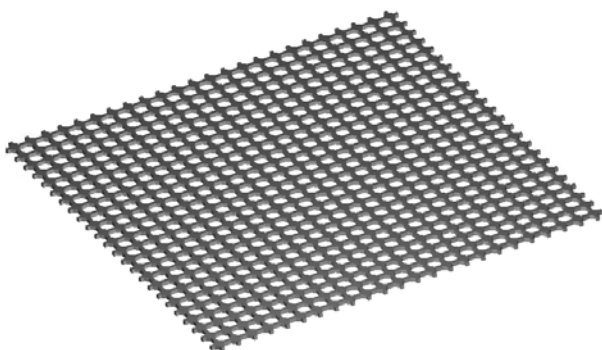


Fig. 3. Schematic view of one fiber layer in the preform

2.4.2 Generating the whole preform

The next step is to position a number of fiber layers in a staggered manner in order to conduct a preform which allows for a realistic propagation of the molten aluminum.

Every second fiber layer is fixed and every other second fiber layer is randomly inserted, see Fig. 4. The distance between two fixed fiber layers is four times the fiber diameter. Thus, the space between adjacent fiber unit nodes in the neighbouring fiber layer is a cube with a side length of four times the fiber diameter. This cube can be divided into 64 small cubes, as the yellow region in Fig. 4 shows. The fiber unit node of the random fiber layer is positioned in the center of one of the small cubes randomly.

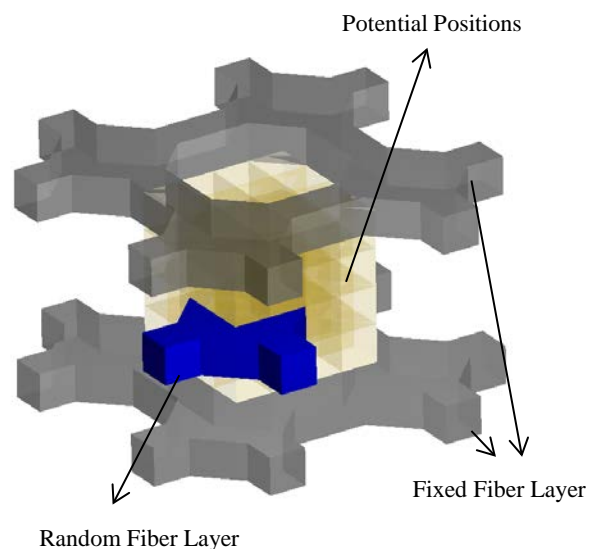


Fig. 4. The placement of the fiber layers

Thus, a fibrous preform which consists of unstructured fiber layers is obtained, see Fig. 5, and the volume fraction of the fibers is approximately 22%.

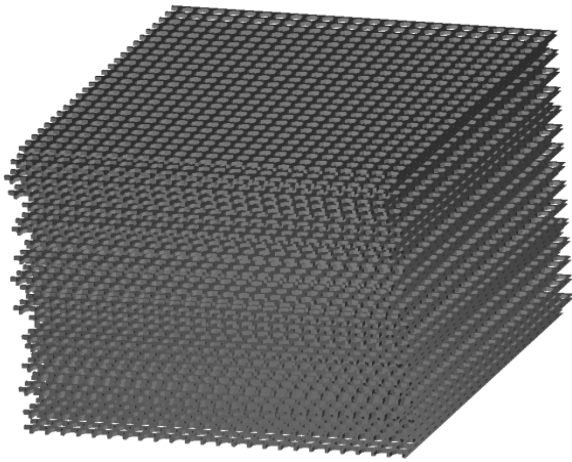


Fig. 5. Schematic view of geometric model of the preform

2.4.3 Importing the preform into FLOW-3D

After the STL file of the preform is created, it is imported into FLOW-3D and trimmed in order to have the same size as the cylindrical mold, see Fig. 6. Note that in this preliminary study, the lengths of all sides of the control volumes are set equal to the fiber diameter in order to decrease the computational load, even though a finer mesh might give more accurate results.

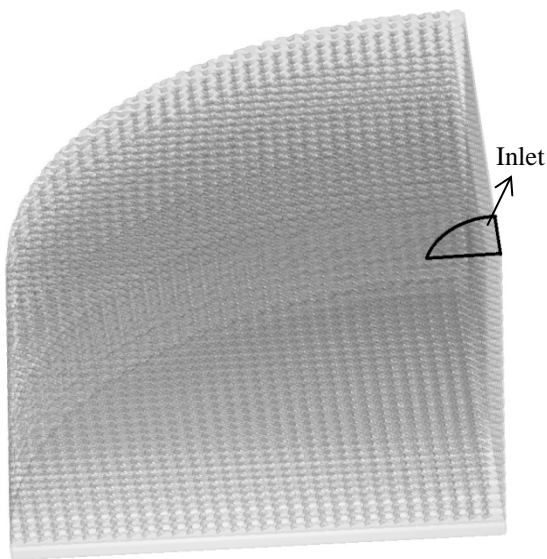
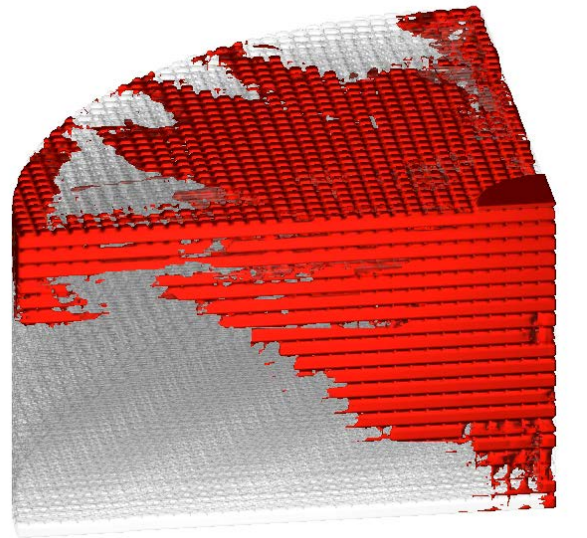


Fig. 6. Computational domain in the CFD model

3 Results and discussion

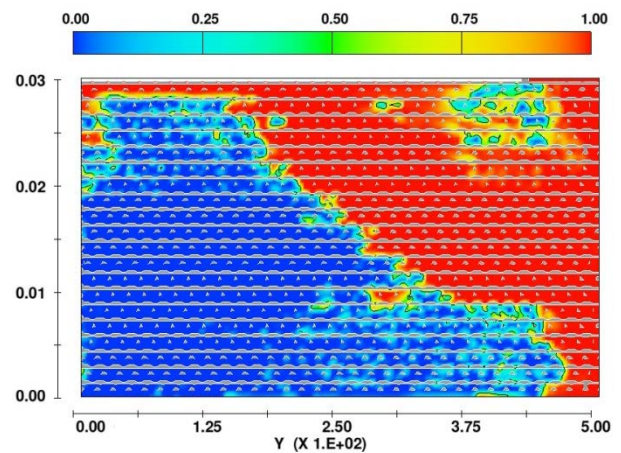
3.1 Flow pattern

In Figs. 7(a) and 8(a), the flow propagation of the molten metal is shown in the case of a fiber diameter size of $300\ \mu\text{m}$ and $200\ \mu\text{m}$, respectively. In the figures, the molten metal is represented with red and the porous preform with grey.



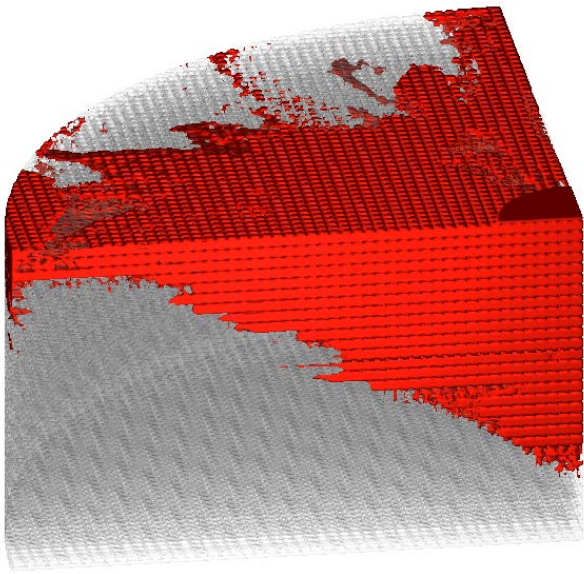
(a)

fraction of fluid contours

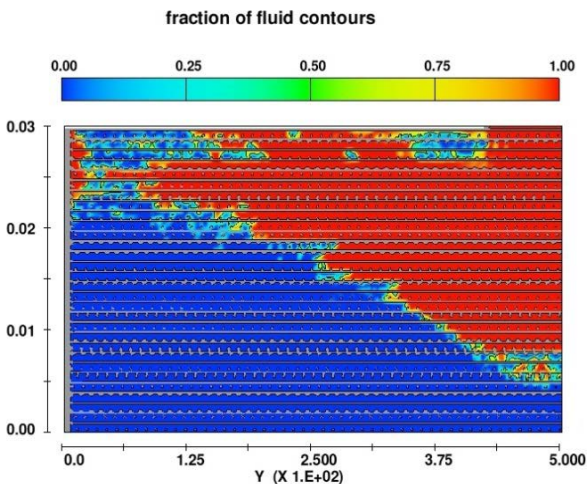


(b)

Fig. 7. Flow propagation of molten aluminum in porous preform with $300\ \mu\text{m}$ fibers. (a) $\frac{1}{4}$ of preform; (b) at the symmetry boundary.



(a)



(b)

Fig. 8. Flow propagation of molten aluminum in porous preform with 200 μm fibers. (a) $\frac{1}{4}$ of preform; (b) at the symmetry boundary.

The observed infiltration pattern is very similar to the one documented in [11] where the experimental validated porous media/permeability approach is utilized. This fact indicates that the presented CFD approach captures the physics involved in the problem correctly. In addition, the simulated flow condition at the symmetry boundary in Figs. 7(b) and 8(b) illustrates that with this approach it is possible to capture local porosities during the

infiltration process. Thus, the numerical model predicts areas of the preform where the risk of unintended porosities is increased. Potentially, this information could be used to analyze the process parameters in order to obtain the flow pattern with the lowest risk of unintended porosities. Ideally, the numerical model would predict unfilled areas of the preform at the end of the infiltration process, but in order to obtain such results one would have to include a thermal calculation. However, that addition has not been considered in this preliminary study.

3.2 Filling time

In Fig. 9 the relationship between the filling time and filling fraction is shown for the simulations where the fiber diameters 300 μm and 200 μm are utilized.

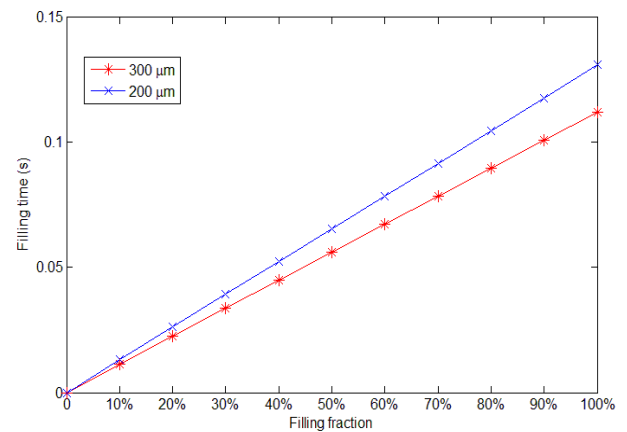


Fig. 9. The relationship between filling time and filling fraction

Both relationships are relatively linear, but the final filling time increases from 0.112 for the 300 μm -fiber-diameter preform to 0.131s for the 200 μm -fiber-diameter preform. The increasing final filling time is an effect of the decreasing permeability when decreasing the size of the fiber diameters in the preform.

In Fig. 10, the relationship between filling time and fiber diameter is shown. Each of the dots represents a simulation and the curve is a best fit function. Note that due to calculation time, the simulations with a fiber diameter of 100 and 50 μm are carried out with

a half and a quarter of the initial diameter and height of the preform, respectively. Afterwards, the two simulations' filling time for the initial size of the preform is found by extrapolation, assuming that their relationship between the filling time and filling fraction are also linear. It is the extrapolated filling times which are documented for the 100 and 50 μm -fiber-diameter preform in Fig. 10. The best fit function illustrates that the filling time increases in an exponential-like manner when decreasing the fiber diameter.

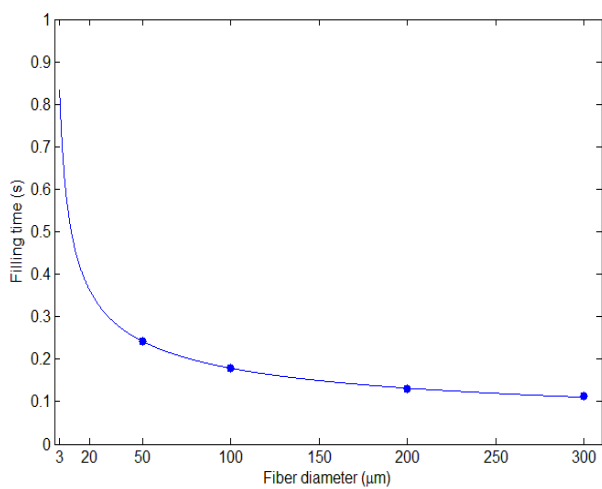


Fig. 10. Relationship between fiber diameter and filling time

The filling time reported in [11] was 20s for a 3 μm -fiber-diameter preform and that differs from the simulated filling time of 0.8s found by the best fit function, see Fig. 10. The difference could be an artifact of the numerical generated preform. One might obtain a simulated filling time which is in better agreement with the experimentally measured filling time if the numerical preform is conducted differently, e.g. introducing inclined fiber layers.

3.3 Calculation time

The number of control volumes increases rapidly when decreasing the fiber diameter as seen in Fig. 11. Consequently, the calculation time increases rapidly too.

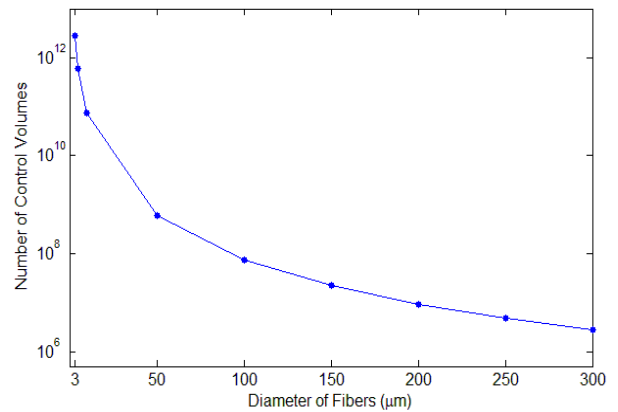


Fig. 11. The relationship between number of control volumes and fiber diameter.

The calculation times of the simulation with the 300 μm -fiber-diameter and 200 μm -fiber-diameter preform were approximately 2 and 6 days, respectively. A simulation with a 3 μm -fiber-diameter preform is therefore not feasible to carry out within a reasonable time frame unless a super computer is utilized. This limitation restricts the CFD approach from being used to simulate the infiltration process of preforms where the size of the reinforcement is much less than 200 μm . However, some metal matrix composites are produced with spherical particles that have a diameter of the order of 100 μm and in such case this numerical approach would be able to analyze the infiltration process if the preform is confined to a quarter of the size of the preform used in this study.

4 Conclusions

In this paper it was shown that a CFD approach has a great potential to simulate the infiltration process and predict unintended porosities in metal matrix composites. Several cases of an infiltration process with an artificially generated fibrous preform are simulated using this approach.

First of all, the simulated flow pattern using this CFD approach is in good agreement with a similar case from literature using a porous media/permeability approach. It shows the capability of the CFD approach to capture local porosities during the infiltration process.

Secondly, the relationship between filling time and fiber diameter of the preform is studied. The final filling time increases when decreasing the size of the fiber diameter in the preform. The filling time with a 3 μm -fiber-diameter preform is 0.8s by extrapolation according to the best fit function based on the simulation results with larger fiber-diameter preform.

Finally, it is not feasible to carry out a simulation with a 3 μm -fiber-diameter preform at present due to the huge amount of control volumes. However, this CFD approach can be used to simulate the infiltration process producing some Metal Matrix Composites with spherical particles which have a diameter of the order of 100 μm .

Of interest in future work is to include a thermal calculation in the CFD approach and try to obtain the volume fraction of air in the end of the infiltration process. Moreover, experimental infiltration tests should be carried out to be compared with the numerical simulation results.

Acknowledgments

The project is part of the VTU Innovation consortium titled "Functionally Optimized Materials" (F.MAT). The support of the China Scholarship Council (CSC) is also gratefully acknowledged.

References

- [1] J. Banhart "Manufacturing, characterization and application of cellular metals and metal foams". *Progress in Materials Science*, Vol. 46(6), pp 559-632, 2001.
- [2] Z. Xia, Y. Zhou, Z. Mao, and B. Shang "Fabrication of Fiber-Reinforce Metal-Matrix Composites by Variable Pressure Infiltration". *Metallurgical Transactions B*, Vol. 23B, pp 195-302, 1992.
- [3] D. K. Biswas, J. E. Gatica, and S. N. Tewari "Dynamic Analysis of Unidirectional Pressure Infiltration of Porous Preforms by Pure Metals". *Metallurgical And Materials Transactions A*, Vol. 29A, pp 377-385, 1998.
- [4] L. J. Masur, A. Mortensen, J. A. Cornie. And M. C. Flemings "Infiltration of Fibrous Preforms by a Pure Metal: Part II. Experiment". *Metallurgical Transactions A*, Vol. 20A, pp 2549-2557, 1989.
- [5] M. Bahraini, J. M. Molina, M. Kida, L. Weber, J. Narciso, and A. Mortensen "Measuring and tailoring capillary forces during liquid metal infiltration". *Current Opinion in Solid State and Materials Science*, Vol. 9, pp 196-201, 2005.
- [6] A. Léger, N. R. Calderon, R. Charvet, W. Dufour, C. Bacciarini, L. Weber, and A. Mortensen "Capillarity in pressure infiltration: improvements in characterization of high-temperature systems". *Journal of Material Science*, Vol. 47, pp 8419-8430, 2012.
- [7] P. K. Rohatgi, J. K. Kim, N. Gupta, S. Alaraj, A. Daoud "Compressive characteristics of A356/fly ash cenosphere composites synthesized by pressure infiltration technique". *Composites Part A: applied science and manufacturing*, Vol. 37, pp 430-437, 2006.
- [8] M. Huang, Y. Wang, F. Wang, J. Gao "Prediction of Critical Pressure in the Preparation of Composites by Vacuum - Pressure Infiltration Process". *Key Engineering Materials*, Vol. 512-515, pp 427-430, 2012.
- [9] K. M. S. Manu, V. G. Resmi, M. Brahmakumar, N. Anand, T. P. D. Rajan, C. Pavithran, B. C. Pai, K. Manisekar "Synthesis of porous SiC preform and squeeze infiltration processing of Aluminium-SiC Metal ceramic composites". *Materials Science Forum*, Vol. 710, pp 371-376, 2012.
- [10] S. Vaidyaraman, W. Lackey, G. Freeman, P. Agrawal, M. Langman "Fabrication of carbon-carbon composites by forced flow-thermal gradient chemical vapor infiltration". *Journal of Materials Research*, Vol. 10, pp 1469-1477, 1995.
- [11] T. Dopler, A. Modaresi and V. Michaud "Simulation of Metal-Matrix Composite Isothermal Infiltration Processing". *Metallurgical And Materials Transactions B*, Vol. 31B, pp 225-234, 2000.
- [12] A. Mortensen, L. J. Masur, J. A. Cornie, and M. C. Flemings. "Infiltration of Fibrous Preforms by a Pure Metal: Part I. Theory". *Metallurgical Transactions A*, Vol. 20A, pp 2535-2547, 1989.
- [13] S. Long, Z. Zhang, and H. M. Flower "Characterization of Liquid Metal Infiltration of a Chopped Fibre Preform Aided by External Pressure II. Modelling of liquid metal infiltration process". *Acta Metallurgical Material*, Vol. 43, pp 3499-3509, 1995.
- [14] Y. Nishida, and G. Ohira "Modelling of Infiltration of Molten Metal in Fibrous Preform by Centrifugal Force". *Acta Materialia*, Vol. 47(3), pp 841-852, 1999.
- [15] E. Lacoste, M. Aboulfatah, M. Danis, and F. Girot "Numerical Simulation of the Infiltration of Fibrous Preforms by a Pure Metal". *Metallurgical Transactions A*, Vol. 24A, pp 2667-2678, 1993.
- [16] P. Li, L. Zeng, B. Wu, X. Cheng, H. Wang, and P. Liu "Simulation of Melting Infiltration Process of

Phase Change Material in Fiber Porous Ceramic".
Materials Science Forum, Vol. 689, pp 198-203,
2011.

[17] Flow3D User's Manual, version 10.1.

[18] <http://www.mathworks.com/matlabcentral/fileexchange/20922-stlwrite-write-binary-or-ascii-stl-file>